sion that contained approximately 2 mM bolyte.

Static Turbidimetry. A 3.00-mL aliquot of the stock analyte containing the suspension of mildly sonicated vesicles was transferred into a quartz cuvette, and the turbidimetric profile at ambient temperature was recorded in the range between 400 and 600 nm, using a Hewlett-Packard Model 8452 A diode array spectrophotometer set with an integration time of 10 s. Deionized water was used as the reference in a cuvette that was matched with respect to that holding the analyte. *Note*: Because absorption spectrophotometers are not ideal turbidimeters, the corresponding turbidance measurements will vary somewhat according to the instrument that is employed.

Vesicle Lysis. After recording the turbidance spectrum, the organizates were disassembled by the addition of about 200 μL of 0.775 M sodium dodecyl sulfate into 3.00 mL of analyte, to give a final concentration of about 0.0500 M in SDS, which is well above the value of its critical micelle concentration of 8.16 mM in water. The electronic absorption spectrum of the clear solution was subsequently recorded in the range between 400 and 600 nm. Observe that the optical densities of the bolyte solutions measured thereby were negligible above 400 and 424 nm, respectively, in the case of bolytes **1** and **7**.

Dynamic Turbidimetry. Laser-light-scattering profiles were recorded by means of a Coulter Model N45D spectrometer equipped with a 632.8-nm helium-neon laser operated at 4 nW. In the case of the large mildly sonicated vesicles, a 2.00-mL aliquot of the suspension was placed in the sample compartment and then allowed to equilibrate thermally with the surroundings for 45 min before the light-scattering profile was recorded. The corresponding measurements of the hydrodynamic diameter as a function of increasing temperature were carried out in sequence using the same stoppered sample, which was thermostated with ±0.2 °C. In a representative experiment, the sample time was set at about 20 μs, the acquisition time was 500 s, and the scattering angle was fixed at 90°.

Transmission Electron Microscopy was also used to detect and measure the vesicles. The respective samples were prepared by fixing the aggregates with osmium tetroxide and then staining them with zinc uranyl acetate. Accordingly, fixation was carried out by adding 1 drop of 4% OsO_4 to 1 mL of the vesicle suspension; upon being allowed to stand at room temperature for 1 h, the mixture was stained with 2% (w/w) uranyl acetate. A drop of the suspension was then placed on a carbon-coated copper grid and blotted dry after 60 s. Finally, the sample was examined by means of a Phillips E.M. 300 electron microscope operated at 60 kV.

Acknowledgment. We thank the NIH for a grant (GM-36262) that supported portions of this work. In addition, S.M. was supported by a NIH Minority Post-doctoral Supplement, for which we are grateful.

Methanolysis of K-Region Arene Oxides: Comparison between Acid-Catalyzed and Methoxide Ion Addition Reactions

Nashaat T. Nashed,*,‡ Ad Bax,† Richard J. Loncharich,§,⊥ Jane M. Sayer,‡ and Donald M. Jerina‡

Contribution from the Laboratories of Bioorganic Chemistry and Chemical Physics, National Institute of Diabetes and Digestive and Kidney Diseases, and Molecular Graphics and Simulation Laboratory, Division of Computer Research and Technology, The National Institutes of Health, Bethesda, Maryland 20892. *Received June 8, 1992. Revised Manuscript Received October 5, 1992*

Abstract: Reactions of K-region arene oxides of benz[*a*]anthracene (BA-O) and its 1- (1-MBA-O), 4- (4-MBA-O), 7- (7-MBA-O), 11- (11-MBA-O), 12-methyl- (12-MBA-O), 7,12-dimethyl-(DMBA-O), and 7-bromo- (7-BrBA-O) substituted derivatives, benzo[a]pyrene (BaP-O), benzo[*c*]phenanthrene (BcP-O), benzo[*e*]pyrene (BeP-O), benzo[*g*]chrysene (BgC-O), chrysene (Chr-O), dibenz[*a,h*]anthracene (DBA-O), phenanthrene (Phe-O), 3-bromophenanthrene (3-BrPhe-O), and pyrene (Pyr-O) with acid and methoxide ion in methanol, are compared. For the acid-catalyzed reaction, products consist of *cis*- and *trans*-methanol adducts and phenols. There is no isotope effect on the ratio of phenols to solvent adducts produced from Phe-O or BcP-O when deuterium is substituted for the hydrogen that migrates. This observation is consistent with a mechanism in which product distribution in acid is determined by the relative rates of solvent capture and conformational inversion of a carbocation intermediate. As expected, only *trans*-methanol adducts, consisting of regioisomeric mixtures for unsymmetrical arene oxides, are formed from the reaction of methoxide ion with K-region arene oxides. The use of methanol permits the identification of products formed at each benzylic position of unsymmetrical arene oxides. Rate data for reactivity at each position could be fitted to the equation $\log k_{MeO}/k_{MeO}^{Phe\text{-}O} = m(\log k_H/k_H^{Phe\text{-}O}) + b$, where k_{MeO} and k_H are the second-order rate constants of the methoxide ion addition and acid-catalyzed reaction, respectively, and $k_{MeO}^{Phe\text{-}O}$ and $k_H^{Phe\text{-}O}$ are the corresponding rate constants for the reference compound phenanthrene oxide. A plot of $\log k_{MeO}/k_{MeO}^{Phe\text{-}O}$ vs $\log k_H/k_H^{Phe\text{-}O}$ for the reaction of 1-MBA-O, 12-MBA-O, DMBA-O, BcP-O, and BgC-O, which have either a methyl substituent in the bay region or a sterically crowded fjord region which affects the planarity of the molecules, defined one line ($m = 0.31 \pm 0.02$, $b = 0.67 \pm 0.09$), whereas a plot of the data for the reaction of the nearly planar arene oxides BA-O, 4-MBA-O, 7-MBA-O, 11-MBA-O, BaP-O, BeP-O, Chr-O, DBA-O, Phe-O, and Pyr-O defined a different line ($m = 0.33 \pm 0.07$, $b = -0.05 \pm 0.05$). The nonzero intercept for the sterically crowded, nonplanar arene oxides indicates a steric acceleration of their rates of methoxide ion addition. The positive slopes of both lines are consistent with an S_N2 mechanism with an unsymmetrical transition state in which the epoxide C–O bond breaking is more advanced than the formation of the new C–O bond to methoxide ion, such that a partial positive charge is developed on the aromatic moiety.

Introduction

Both benzo-ring and K-region arene oxides are common mammalian metabolites of the environmentally ubiquitous polycyclic aromatic hydrocarbons.[1a] These inherently cytotoxic and genotoxic metabolites are initially formed by the action of the cytochromes P450 and are subsequently transformed into *trans*-dihydrodiols and glutathione conjugates by microsomal xenobiotic epoxide hydrolase and the cytosolic glutathione *S*-transferases, respectively. In both cases, these enzymes display substantial enantio- and regioselectivity toward arene oxide substrates.[1-3] Detailed understanding of their mechanisms of

* Address correspondence to Dr. Nashaat T. Nashed, National Institutes of Health, Bldg. 8, Room 1A02, Bethesda, MD 20892, Tel. (301)-496-1780, Fax (301)-402-0008.

‡ Laboratory of Bioorganic Chemistry.

† Laboratory of Chemical Physics.

§ Molecular Graphics and Simulation Laboratory.

⊥ Current address: Supercomputer Applications and Molecular Design, Eli Lilly and Company, Lilly Corporate Center, Indianapolis, IN 46285-0403.

(1) (a) Boyd, D. R.; Jerina, D. M. In *Small Ring Heterocycles*; Hassner, A., Ed.; John Wiley and Sons, Inc.; New York, 1985; Vol. 42, Part 3, pp 197-282. (b) Armstrong, R. N. *Chem. Res. Toxicol.* **1991**, *4*, 131.

0002-7863/93/1515-1711$04.00/0

Scheme I

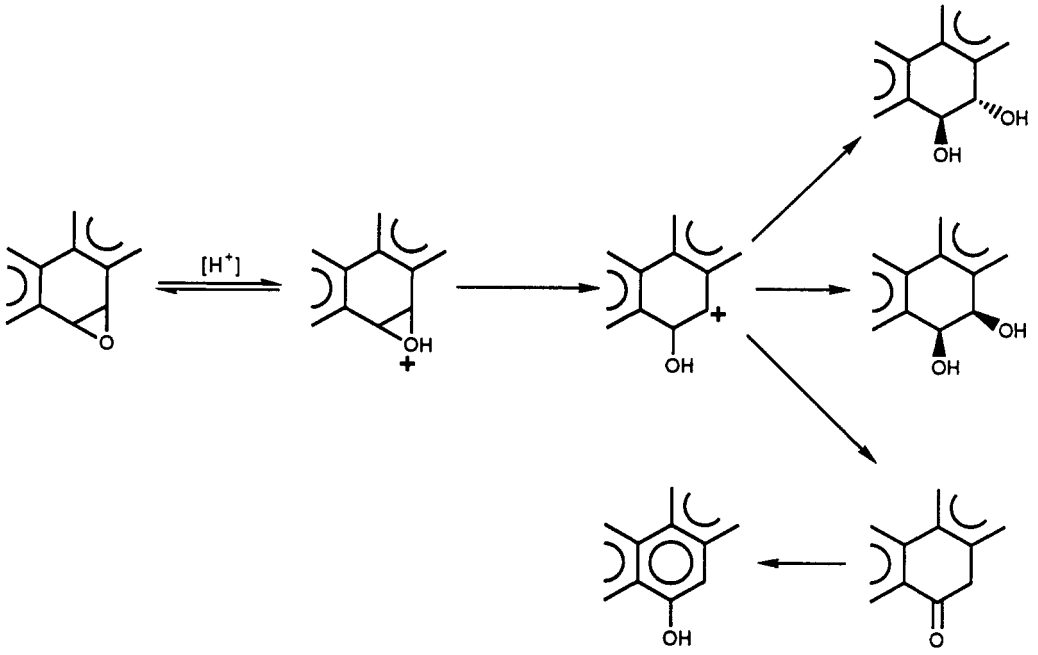

action would be greatly enhanced through increased knowledge of the chemical reactivity of arene oxide substrates. For example, differences in the intrinsic chemical reactivities of the two epoxide centers of an unsymmetrical arene oxide probably contribute significantly to the observed enzymatic regioselectivity and may mask the contribution of the active site geometry to this regioselectivity. The present study examines reactions of a wide range of K-region arene oxides (Figure 1) with acid and methoxide ion in methanol in order to obtain a detailed understanding of the intrinsic chemical reactivities of the two benzylic epoxide centers in unsymmetrical K-region arene oxides. Methanolysis was selected because it allows facile determination of the relative chemical reactivities of both epoxide centers since solvent adducts are isomeric dihydrodiol monomethyl ethers whose structures are readily characterized.

The acid-catalyzed solvolysis reaction of K-region arene oxides in aqueous solutions has been the subject of several mechanistic investigations.[4-12] Bruice and co-workers investigated the acid-catalyzed solvolysis of phenanthrene 9,10-oxide (Phe-O) in aqueous solutions and proposed the carbocation mechanism shown in Scheme I.[4,5] The acid-catalyzed solvolyses of Phe-O[5,6] and substituted derivatives,[5,7,8] benz[*a*]anthracene 5,6-oxide (BA-O),[5,9a] dibenz[*a*,*h*]anthracene 5,6-oxide (DBA-O),[9a] 3-methylcholanthrene 11,12-oxide,[9a] 7,12-dimethylbenz[*a*]anthracene 5,6-oxide (DMBA-O),[9b] and pyrene 4,5-oxide (Pyr-O)[5] in aqueous solutions and benzo[*a*]pyrene 4,5-oxide (BaP-O) in methanol[10] have been examined, and the results are consistent with the mechanism in Scheme I. However, the effect of structure on the relative reactivities of the two epoxide centers and on the partitioning of the carbocation intermediates to adducts and phenols have not been addressed. Recently, the acid-catalyzed solvolysis reactions of BA-O and its methyl and bromine substituted derivatives (cf. Figure 1) have been examined in 1:9 dioxane–water and in methanol.[11] Although acid-catalyzed reaction rates in methanol range from 3- to 8-fold higher than in 1:9 dioxane–water, relative reactivites of both epoxide centers as well as effects of structure on product distributions are similar in both solvents. Therefore, it is concluded that the mechanism of reaction in both solvents is very similar. In this study and the following paper in this issue,[12] we extend our observations of the effect of structure on reactivity and product distribution for the acid-catalyzed reactions of K-region arene oxides (cf. Figure 1) in methanol and the nonnucleophilic solvent acetonitrile.

K-region arene oxides undergo trans addition reactions with nitrogen, oxygen, and sulfur nucleophiles in aqueous and organic solvents.[8,10,13-16] Reaction of methoxide ion with several K-region arene oxides has been reported without kinetic analysis.[17-19] In the present study, we report kinetics and product distributions for the reaction of methoxide ion with K-region arene oxides shown in Figure 1. Our results show that the methoxide ion addition is sensitive to electronic effects that parallel those for the corresponding acid-catalyzed methanolysis reactions as well as to steric effects arising from crowding in remote bay-region or fjord-region positions.

Results and Discussion

Mechanism of Acid-Catalyzed Methanolysis of K-Region Arene Oxides. The mechanism shown in Scheme II is proposed to account for the results described for the acid-catalyzed methanolysis of BA-O and substituted derivatives[11] as well as K-region arene oxides derived from other hydrocarbons described in this study (cf. Tables I and II). The following salient features of this mechanism are supported by experimental evidence in this and

(2) van Bladeren, P. J.; Sayer, J. M.; Ryan, D. E.; Thomas, P. E.; Levin, W.; Jerina, D. M. *J. Biol. Chem.* **1985**, *260*, 10226.
(3) Yang, S. K. *Biochem. Pharm.* **1988**, *37*, 61.
(4) Bruice, T. C.; Bruice, P. Y. *Acc. Chem. Res.* **1976**, *9*, 378.
(5) Bruice, P. Y.; Bruice, T. C.; Dansette, P. M.; Selander, H. G., Yagi, H.; Jerina, D. M. *J. Am. Chem. Soc.* **1976**, *98*, 2965.
(6) Whalen, D. L.; Ross, A. M.; Dansette, P. M.; Jerina, D. M. *J. Am. Chem. Soc.* **1977**, *99*, 5672.
(7) Darnow, J. N.; Armstrong, R. N. *J. Am. Chem. Soc.* **1990**, *112*, 6725.
(8) Okamoto, T.; Shudo, K.; Miyata, N.; Kitahara, Y.; Nagata, S. *Chem. Pharm. Bull.* **1978**, *26*, 2014.
(9) (a) Keller, J. W.; Heidelberger, C. *J. Am. Chem. Soc.* **1976**, *98*, 2328. (b) Keller, J. W.; Kundu, N. G.; Heidelberger, C. *J. Org. Chem.* **1976**, *41*, 3487.
(10) Hylarides, M. D.; Lyle, T. A.; Daub, G. H.; Jagt, D. L. V. *J. Org. Chem.* **1979**, *44*, 4652.
(11) Nashed, N. T.; Balani, S. K.; Loncharich, R. J.; Sayer, J. M.; Shipley, D. Y.; Mohan, R. S.; Whalen, D. L.; Jerina, D. M. *J. Am. Chem. Soc.* **1991**, *113*, 3910.
(12) Nashed, N. T.; Sayer, J. M.; Jerina, D. M. following paper in this issue.
(13) Bruice, P. Y.; Bruice, T. C.; Yagi, H.; Jerina, D. M. *J. Am. Chem. Soc.* **1976**, *98*, 2973.
(14) Balani, S. K.; Sayer, J. M.; Jerina, D. M. *J. Am. Chem. Soc.* **1989**, *111*, 3290.
(15) Beland, F. A.; Harvey, R. G. *J. Am. Chem. Soc.* **1976**, *98*, 4963.
(16) Posner, G. H.; Lever, J. R. *J. Org. Chem.* **1984**, *49*, 2029.
(17) Balani, S. K.; van Bladeren, P. J.; Cassidy, E. S.; Boyd, D. R.; Jerina, D. M. *J. Org. Chem.* **1987**, *52*, 137.
(18) Weems, H. B.; Mushtaq, M.; Yang, S. K. *Anal. Chem.* **1987**, *59*, 2679.
(19) Yang, S. K.; Mushtaq, M.; Weems, H. B.; Miller, D. W.; Fu, P. P. *Biochem. J.* **1987**, *245*, 191.

Scheme II

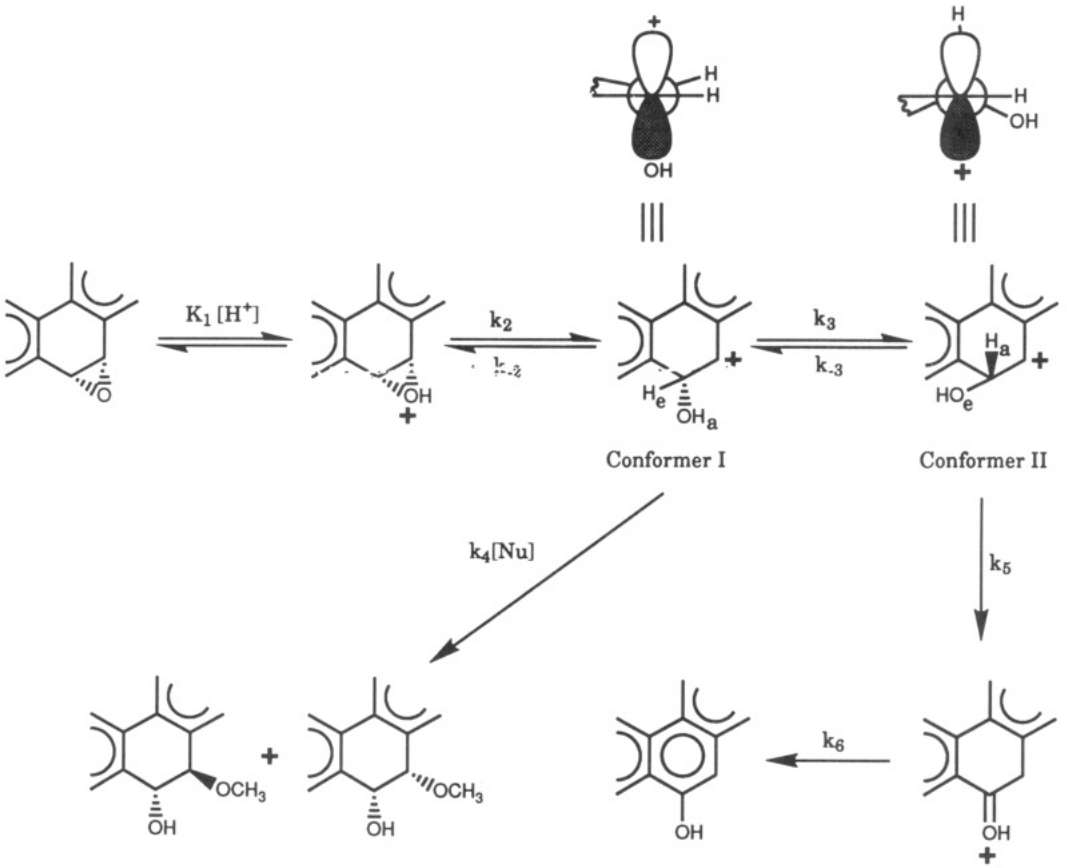

previous work.[11] (**1**) Upon acid catalyzed ring cleavage, the oxirane opens to an initial carbocation (conformer I) which represents a true intermediate (i.e., a local energy minimum) and which has the *hydroxyl group in a pseudoaxial orientation.* Although two distinct regioisomeric carbocations may be formed from unsymmetrical arene oxides, the initial conformation of each cation must be the one in which the hydroxyl group is pseudoaxial. This conformation yields exclusively cis and trans products derived from trapping by solvent. (**2**) The interconversion of conformer I of the carbocation and the alternative conformer II, in which the *hydrogen on the hydroxyl-bearing carbon is pseudoaxial*, occurs at a rate that is kinetically significant relative to the rates of processes leading to products. (**3**) Conformer II yields phenolic products exclusively, presumably by a pathway involving migration of the pseudoaxial hydrogen.

Axial opening of the protonated oxirane to conformer I,[11] which may or may not be the thermodynamically preferred conformer, should be favored kinetically by the principle of least motion. Conversion of conformer I to II requires rotations around both the K-region and biphenyl bonds (cf. Scheme II). Support for a significant energy barrier for the interconversion of conformers I and II when these rotations are sterically restricted was provided both by theoretical calculations and by the observation that little or no phenols are formed from substituted benz[*a*]anthracene 5,6-oxides with bulky methyl substituents in the bay region.[11] Thus, steric hindrance to conformational isomerization (k_3 slow) results in a preponderance of reaction via the alternative pathway k_4[Nu]. Furthermore if conformer II is *thermodynamically unstable* relative to I, the yield of phenol should be small. Formation of phenols is expected to be more favorable from conformer II than from I, because the bond to the migrating hydrogen is nearly periplanar with the vacant p-orbital of conformer II, whereas it is nearly orthogonal to this orbital in conformer I. In derivatives of BA-O, a methyl substituent peri to the hydroxyl group of the carbocation intermediate destabilizes conformer II in which this hydroxyl group is pseudoequatorial and the corresponding hydrogen is pseudoaxial; thus, diminished yields of phenols with a peri methyl substituent were ascribed to the difficulty of assuming this conformation.

Table I. Product Distributions for the Acid-Catalyzed Methanolysis of K-Region Arene Oxides

arene oxide	% product from each carbocation		addition products % trans	addition products % cis	phenol	ratio[a]
Chr-O	C_5	93	5		88	17.6
	C_6	7	6	1	trace[b]	<0.07[c]
BgC-O	C_9	88	12	3	73	4.9
	C_{10}	12	12			
BcP-O	C_5	13	7		6	0.86
	C_6	87	42	1	44	1.02
BcP-O-d[d]	C_5	14	6		8	1.3
	C_6	86	42	2	42	0.96
BA-O[e]	C_5	37	23	6	8	0.28
	C_6	63	38	9	16	0.34
DBA-O[f]	C_5	24	15	2	7	0.41
	C_6	76	38	18	20	0.36
BaP-O[f]	C_4	45	20	7	18	0.67
	C_5	55	26	8	21	0.62
Phe-O	C_9	100	54	9	37	0.59
Phe-O-9,10-d_2	C_9	100	57	8	35	0.53
BeP-O	C_4	100	48	9	43	0.75
Pyr-O	C_4	100	47	9	44	0.79
3-BrPhe-O	C_9	53	34	3	16	0.43
	C_{10}	47	27	4	16	0.52

[a] Ratio of phenol to cis and trans addition products. [b] <0.5%. [c] The ratio is calculated based on 0.5% of phenol formed. [d] Deuterated 50% at C_5 and C_8. [e] Data from ref 11. [f] Product compositions were unchanged after 1, 3, and 6 half-lives.

The present results provide a number of new observations that support the mechanism of Scheme II and illustrate its generality in systems other than the substituted BA-O series. For example, solvolysis of BgC-O yielded only one phenol (Table I), namely the one derived from the bay-region carbocation, whose positive charge is at C_9 and whose phenolic hydroxyl group is in a non-

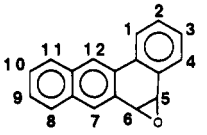

Benz[a]anthracene 5,6-oxide (**BA-O**)
1-Methylbenz[a]anthracene 5,6-oxide (**1-MBA-O**)
4-Methylbenz[a]anthracene 5,6-oxide (**4-MBA-O**)
7-Bromobenz[a]anthracene 5,6-oxide (**7-BrBA-O**)
7-Methylbenz[a]anthracene 5,6-oxide (**7-MBA-O**)
11-Methylbenz[a]anthracene 5,6-oxide (**11-MBA-O**)
12-Methylbenz[a]anthracene 5,6-oxide (**12-MBA-O**)
7,12-Dimethylbenz[a]anthracene 5,6-oxide (**DMBA-O**)

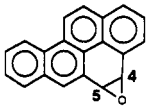

Benzo[a]pyrene 4,5-oxide (**BaP-O**)

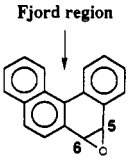

Benzo[c]phenanthrene 5,6-oxide (**BcP-O**)

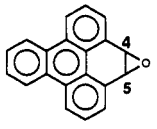

Benzo[e]pyrene 4,5-oxide (**BeP-O**)

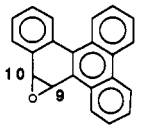

Benzo[g]chrysene 9,10-oxide (**BgC-O**)

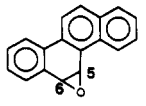

Chrysene 5,6-oxide (**Chr-O**)

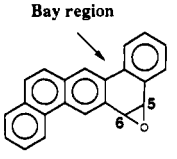

Dibenz[a,h]anthracene 5,6-oxide (**DBA-O**)

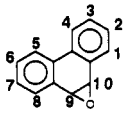

Phenanthrene 9,10-oxide (**Phe-O**)
3-Bromophenanthrene 9,10-oxide (**3-BrPhe-O**)

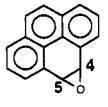

Pyrene 4,5-oxide (**Pyr-O**)

Figure 1. Structures and abbreviations for the studied K-region arene oxides. Examples of bay and fjord regions are indicated.

bay-region position. Also, the C_5 carbocation derived from Chr-O, which has the hydroxyl group in a non-bay-region position, produced mostly 6-hydroxychrysene, whereas the C_6 carbocation, which has its hydroxyl group in the bay region, yielded predominantly solvent addition products and only a trace of 5-hydroxychrysene. These results are consistent with a mechanism described for the solvolyses of 4-MBA-O and 7-MBA-O.[11] In the present compounds, the steric influence of the bay region resembles that of the peri-methyl group and leads to a strongly diminished tendency for phenol formation from carbocations in which the hydroxyl group is in such a sterically restricted environment. Furthermore, the lower stability of a non-bay-region carbocation relative to a bay-region carbocation may result in a faster rate for solvent trapping (k_4) relative to conformational inversion.

Energy Barriers to Conformational Isomerization. New findings in this work provide further support for the role of conformational isomerization in product determination. The observation (Table I) that there is no deuterium isotope effect on product distribution from 9,10-$^2H_2$-Phe or BcP-O 50% deuterated at C_5 indicates that products are determined by a competition between two processes, *neither of which involves migration of the deuterium*. The kinetic isotope effect for the hydride migration step is estimated to be at least 2.[4] If adduct formation and hydride migration were competing directly for a common intermediate (or a pair of intermediates in rapid equilibrium with each other), the ratio of adducts to phenol from Phe-O should increase from ca. 2:1 to ca. 4:1 upon deuterium substitution. Thus, we conclude that product distribution between adducts and phenol is determined by the relative rates of solvent attack on and conformational inversion of carbocation I and that the process k_{-3} that converts conformer II back to I must be slow relative to hydride migration (k_5); in other words, once conformer II is formed it is "committed" to undergo hydride migration. It is also of interest that there is no deuterium isotope effect on the ratio of cis adduct to phenol. This observation requires that hydride migration and cis adduct formation are not competitive processes involving conformer II. The most likely mechanism for cis adduct formation thus involves attack of solvent on conformer I from the same side as that of the carbocation hydroxyl group.

In order to understand the effect of structure on the conformational isomerization step, *cis*- and *trans*-dihydrodiols and their methyl ether derivatives can be used as models for the hydroxy carbocations derived from ring opening of arene oxides. In the absence of *local* steric effects, *trans*-dihydrodiols[11,20-22] and their methyl ethers (cf. Table VI and Experimental Section) generally prefer a pseudodiequatorial orientation for their oxygen substituents, with characteristic coupling constants of 7–10 Hz between the two carbinol protons. On the other hand, in the presence of local steric hindrance due to a peri substituent or adjacent bay region, the *trans*-dihydrodiols and their methyl ethers prefer the pseudodiaxial orientation ($J_{\text{K-region}}$ 3–4 Hz) that minimizes this steric hindrance (i.e., K-region derivatives of DMBA, 4-MBA, and 7-MBA[11] as well as those of BgC[23] and Chr,[17] Table VI). Further examples of these sterically enforced conformational preferences is found from complete analysis of the coupling constants of *cis*-dihydrodiols on benzo-rings where the diol is part of a bay region[21] and from the X-ray crystal structure of DMBA *cis*-5,6-dihydrodiol.[24] In both cases the hindered hydroxyl group, either in the bay region or peri to the C_7 methyl substituent, is pseudoaxial, whereas the other hydroxyl group is pseudoequatorial. A hydroxy carbocation in which the hydroxyl group is in a sterically hindered position such as a bay region or peri to a large substituent would be subject to the same steric effect and should hence prefer a pseudoaxial orientation for the hydroxyl group (conformer I). The effect of such conformational restriction will be to decrease the equilibrium constant (k_3/k_{-3}), the rate constant (k_3), or both. Thus either k_3 or k_3k_5/k_{-3} will become small relative to the solvent trapping rate, k_4[Nu], and the predominant products will arise from solvent addition to conformer I. In accordance with this mechanism, carbocations with their hydroxyl group in a bay region or in a position peri to a bulky substituent produced only addition products, whereas their regioisomeric carbocations, which are not sterically restricted, yielded both solvent adducts and phenols (cf. Table I and ref 11).

We next consider the effect of steric hindrance *remote from the K-region*, which influences predominantly the *rate* of conformational isomerization in these systems due to restricted rotation around the biphenyl bond. K-region *cis*-dihydrodiols and their dimethyl ethers with one pseudoaxial and one pseudoequatorial oxygen substituent provide models for the investigation of these kinetic effects. The conformational interchange (ax,eq

(20) Sayer, J. M.; van Bladeren, P. J.; Yeh, H. J. C.; Jerina, D. M. *J. Org. Chem.* **1986**, *51*, 452.
(21) Jerina, D. M.; Selander, H.; Yagi, H.; Wells, M. C.; Davey, J. F.; Mahadevan, V.; Gibson, D. T. *J. Am. Chem. Soc.* **1976**, *98*, 5988.
(22) Lehr, R. E.; Schaefer-Ridder, M.; Jerina, D. M. *J. Org. Chem.* **1977**, *42*, 736.
(23) Bushman, D. R.; Grossman, S. J.; Jerina, D. M.; Lehr, R. E. *J. Org. Chem.* **1989**, *54*, 3533.
(24) Zacharias, D. E.; Glusker, J. P.; Harvey, R. G.; Fu, P. P. *Cancer Res.* **1977**, *37*, 775.

Table II. Second-Order Rate Constants[a,b] and Partial Rate Constants at Each Epoxide Center for the Acid-Catalyzed Methanolysis of K-Region Arene Oxides

arene oxide	10^{-2} k_H, M^{-1} s^{-1}	position	10^{-2} k_{major}, M^{-1} s^{-1}	position	10^{-2} k_{minor}, M^{-1} s^{-1}
Chr-O	13.70	C_5	12.74	C_6	0.96
BgC-O	11.30	C_9	9.94	C_{10}	1.36
BcP-O	8.23	C_6	7.16	C_5	1.07
BA-O[c]	4.76	C_6	3.00	C_5	1.76
DBA-O	4.24	C_6	3.22	C_5	1.02
BaP-O	4.31	C_5	2.37	C_4	1.94
Phe-O	1.96	C_9	0.98		
BeP-O	1.76	C_4	0.88		
Pyr-O	1.71	C_4	0.86		
3-BrPhe-O	0.408	C_9	0.216	C_{10}	0.192

[a] At 25 °C in 2% (v/v) acetonitrile in methanol. [b] Standard deviations were 2–5% of the reported values. [c] Results from ref 11.

Table III. Conformational Energy Barriers at the Coalescence Temperature for K-Region *cis*-Dihydrodiol Dimethyl Ethers[a]

hydrocarbon	coalescence temp, °C	k,[b] s^{-1}	$\Delta G^{\ddagger}$, kcal/mol
BaP	−32	469	11.1
BA	−20	381	11.8
BcP	+35	326	13.9
12-MBA	+55	272	15.6

[a] In methanol. [b] Rate of exchange at coalescence temperature.

$\rightleftharpoons$ eq,ax) is analogous to the interconversion of conformers I and II of the carbocation in that it requires rotation around both the biphenyl and K-region bonds. When methyl substituents are present in the bay region of substituted benz[*a*]anthracenes (1-MBA and 12-MBA) or when the bay region is replaced by a highly hindered fjord region (BcP), the K-region protons of the 5,6-dihydrodiol dimethyl ethers exhibit broad NMR resonance lines at ambient temperature. This observation indicates that the conformational interchange in solution (5_{ax}, $6_{eq} \rightleftharpoons 5_{eq}$, 6_{ax}) is slow. Other *cis*-dihydrodiol dimethyl ethers that lack unusual steric congestion in the bay region display a single sharp resonance for each proton under the same conditions. At lower temperatures, the broad resonances in the *cis*-5,6-dihydrodiol dimethyl ethers derived from BcP and 12-MBA become sharp, and signals corresponding to the individual conformers can be distinguished. Equal amounts of both conformational isomers are observed indicating no thermodynamic preference for either conformational isomer. Table III summarizes the energy barriers for conformational inversion of the *cis*-dihydrodiol dimethyl ethers of BA, BaP, BcP, and 12-MBA calculated at their coalescence temperatures. The energy barrier for conformational isomerization of the *cis*-dihydrodiol dimethyl ether of 12-MBA is the highest, followed by BcP, and both are significantly higher than those for BA and BaP. The higher energy barriers for the conformational change of BcP and 12-MBA derivatives may be ascribed to the increase of steric interaction between H_1 and H_{12} in the BcP system, and H_1 and the C_{12} methyl substituent in the 12-MBA system, as the hydrocarbon assumes a planar transition structure in passing from one conformer to the other. The observed difference between the energy barrier for the dimethyl ethers of BA and 12-MBA in Table III is 3.8 kcal/mol. This represents a lower limit on the effect of bay-region methyl substitution on the energy barrier because the barriers for the two compounds were determined at different temperatures.

A planar transition structure would also be on the pathway from carbocation conformer I to II, and steric effects of a bay-region substituent or crowded fjord region would hence be expected to raise the energy barrier for the conformational isomerization step (k_3, k_{-3}). Such an increase, relative to the energy barrier for solvent trapping (k_4[Nu]) of conformer I of the carbocation, would favor the formation of addition products. These considerations based on the study of model compounds are consistent with results of calculations on the carbocations themselves. Molecular modeling of both K-region carbocations of BA shows a nearly planar

Chart I

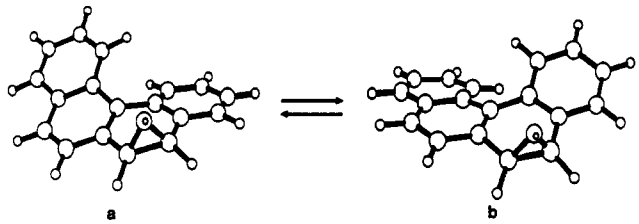

Chart II. Structures of Carbocations Derived from BcP-O

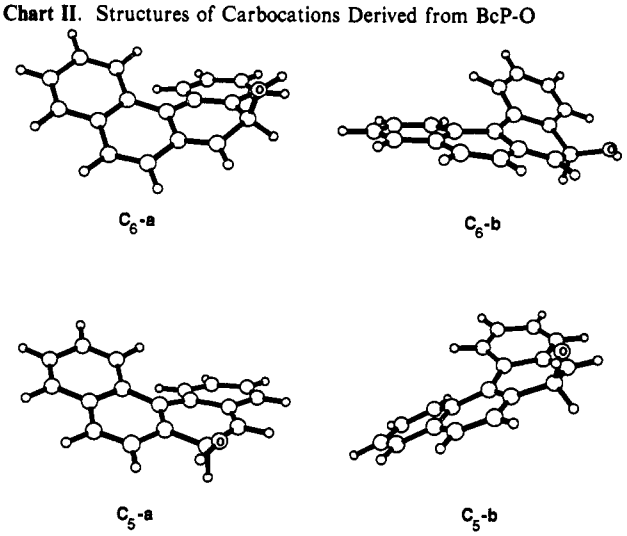

structure for both conformational isomers.[11] On the other hand, the conformational isomers of 12-MBA carbocations are twisted around the biphenyl bond with a dihedral angle around 28°. Only solvent adducts are formed on solvolysis of BA-O derivatives with methyl substituents in the bay region, namely, DMBA-O, 1-MBA-O, and 12-MBA-O,[11] whereas significant amounts of phenolic products are observed from each carbocation derived from BA-O or 11-MBA-O, which lack steric hindrance in the bay region and consequently can undergo more rapid isomerization to conformer II.

BcP-O and Its Carbocations. A situation similar to that of 1- and -12-methyl BA oxides might be expected to apply in the case of K-region arene oxides with a fjord region such as BcP-O and BgC-O. Theoretical and crystallographic studies have shown that BcP and its derivatives are nonplanar due to steric interaction between H_1 and H_{12}.[25,26] A similar steric interaction between H_1 and H_{14} is found in the BgC system. Dewar's AM1 calculations[27] using the MOPAC 4.0 program[28] gave two nonplanar conformational isomers a and b for BcP-O (cf. Chart I) and 12-MBA-O;[11] results are summarized in Table IV. In accordance with the notation used for the BA system,[11] the a and b notations refer, respectively, to negative and positive values of the dihedral angle, C_{12a}–C_{12b}–C_{12c}–C_1, in the BcP system. The structures calculated for the two conformational isomers of BcP-O, **a** and **b** with relative energies of 0.0 and 0.6 kcal/mol, and C_{12a}–C_{12b}–C_{12c}–C_1 dihedral angles of −22.6° and 23.2°, respectively, are similar to those calculated for 12-MBA-O with dihedral angles C_{12}–C_{12a}–C_{12b}–C_1 of −24.2° and 24.3°, respectively.

Structures of carbocations derived from BcP-O were fully optimized with ab initio gradient techniques[29] using the minimal STO-3G basis set.[30] Calculations were performed on the IBM

(25) (a) Hirshfeld, F. L.; Sander, S.; Schmidt, G. M. J. *J. Chem. Soc.* **1963**, 2108. (b) Bernstein, J.; Regev, H.; Herbstein, F. H. *Acta Crystallogr. Sec. B* **1977**, *33*, 1716.

(26) Silverman, B. D. *Cancer Biochem. Biophys.* **1982**, *6*, 23.

(27) Dewar, M. J. S.; Zoebisch, E. G.; Healy, E. F.; Stewart, J. J. P. *J. Am. Chem. Soc.* **1985**, *107*, 3902.

(28) Stewart, J. J. P.; Seiler, F. J. MOPAC, Ver. 4.0, QCPE No. 560, Indiana University, Bloomington, IN.

(29) Hehre, W. J.; Radom, L.; Schleyer, P. v. R.; Pople, J. A. *Ab Intio Molecular Orbital Theory*; John Wiley & Sons: New York, 1986.

Table IV. Relative Energies Calculated for BcP-O and 12-MBA-O and Their Derived Carbocations and *cis*-Dihydrodiols

		BcP		12-MBA	
structure	computational level	C_{12a}–C_{12b}–C_{12c}–C_1 torsional angle	E (rel), kcal/mol	C_{12}–C_{12a}–C_{12b}–C_1 torsional angle	E (rel), kcal/mol
		Arene Oxide			
a	AM1	−22.6	0.0	−24.2	0.0[a]
b	AM1	23.2	0.6	24.3	0.4[a]
		Carbocation[b,c]			
C_6-a	RHF/STO-3G	−27.2	0.0	−29.9[d]	0.0
C_6-b	RHF/STO-3G	26.6	0.2	29.3[d]	0.3
C_5-a	RHF/STO-3G	−22.1	7.6	−23.3[d]	3.1
C_5-b	RHF/STO-3G	23.5	7.7	26.0[d]	2.5
C_6-f	RHF/STO-3G	0.0	11.4	0.0	8.6[e]
C_6-f	RHF/STO-3G			0.0	10.4[f]
C_6-f	AM-1	0.0	10.4	0.0	6.8[e]
		cis-Dihydrodiol			
5ax, 6eq	AM1	−33.9	0.0	−34.3	3.8
5eq, 6ax	AM1	33.3	3.4	34.1	0.0
planar	AM1	0.0	11.6	0.0	9.5[e]
	AM1			0.0	13.0[f]

[a] Note that the energy difference between the conformational isomers of 12-MBA-O is 0.4 kcal/mol using the AM1 calculation. These results are parallel to the results reported in ref 11 obtained by PCMODEL PI calculation. [b] STO-3G bond lengths and angles for carbocations derived from BcP-O are in the supplementary material. [c] The C^+–C–O–H dihedral angle is 180°. [d] Results from ref 11. [e] H_1 is flanked by two hydrogens of the methyl group. [f] The methyl group is rotated by 60° to prevent the interdigitation of H_1 between the methyl hydrogen.

3090-300E vector facility using GAUSSIAN 88 program[31a,b] or on the CRAY-2 using GAUSSIAN 90 program.[31c] The relative energies and C_{12a}–C_{12b}–C_{12c}–C_1 dihedral angles calculated for the two conformations of each carbocation are summarized in Table IV. The corresponding results for the carbocations derived from 12-MBA-O[11] are also included in Table IV for comparison. Bond lengths and angles for carbocations derived from BcP-O are provided in the supplementary material. These carbocations (cf. Chart II) are structurally similar to those derived from 12-MBA-O in that they are highly twisted around the biphenyl bond. Both conformational isomers of the C_6 carbocation, C_6-a and C_6-b, are of comparable energy, 0.0 and 0.2 kcal/mol, with dihedral angles C_{12a}–C_{12b}–C_{12c}–C_1 of −27.2° and 26.6°, respectively. They are ca. 7.5 kcal/mol more stable than the regioisomeric cations C_5-a and C_5-b, which have dihedral angles of −22.1° and 23.5°, respectively. In qualitative agreement with the calculations, 87% of the products of acid-catalyzed methanolysis of BcP-O are derived from the C_6 carbocation (cf. Table I) which is calculated to be the more stable.

On the basis of the above considerations as well as the NMR studies of model *cis*-dihydrodiol dimethyl ethers, we anticipated that the energy barriers for conformational isomerization of both regioisomeric carbocations derived from BcP-O would be comparable to those in the 12-MBA system. Somewhat surprisingly, however, 50% phenolic products are observed from each carbocation derived from BcP-O and 83% of phenol is obtained from the C_9 carbocation derived from BgC-O. This could possibly result from equatorial opening of the protonated epoxide ring to give conformer II directly or loss of a pseudoequatorial proton from carbocation conformer I. These possibilities are regarded as unlikely, since no phenolic products that could be ascribed to such a mechanism are observed in the acid-catalyzed methanolysis reaction of 12-MBA-O,[11] and a different mechanism for the solvolysis of BcP-O is improbable. In addition, a mechanism that involves the loss of a proton from carbocation conformer I would be expected to have a similar conformational requirement to that of the 1,2-hydride shift, in which the C–H bond is periplanar to the empty p-orbital. In a related system where the hydrogen that would either migrate to give ketone or be abstracted to give enol is constrained in a pseudoequatorial orientation, no ketone (enol) is formed by either mechanism.[32] Furthermore, direct observation of the intermediate ketones is possible under solvolytic conditions, and the kinetics of their formation and enolization are consistent with this reaction pathway being the sole route for phenol formation.[12]

We next considered the more attractive possibility that specific electronic effects, unique to each aromatic hydrocarbon, could stabilize the planar transition structure on the path from carbocation conformer I to II and thus influence the magnitude of k_3. It should be noted that the *cis*-dimethyl ethers are not a perfect model for the hydroxy carbocations, since the transition state for the conformational isomerization of the carbocations will gain extra resonance stabilization relative to the individual conformers I or II, because of its planarity which permits the empty p-orbital to interact with the π-system of the neighboring aromatic ring and improves the delocalization between the two aromatic moieties. This resonance stabilization of the planar carbocation structure, which is not relevant to the mechanism for conformational inversion of the dimethyl ethers, could partially compensate for increased steric hindrance in the transition state. As a consequence, the more effectively such delocalization energy can be provided by an aromatic system, the lower the energy barrier will be and the more phenolic product will be formed. Thus, the nature of the hydrocarbon might have a pronounced effect on the height of the energy barrier for the k_3 process.

In order to investigate this possibility, calculations were used to estimate the energy barriers for the conformational isomerization of the carbocations and *cis*-dihydrodiols derived from 12-MBA-O and BcP-O. The transition state for conformational isomerization was assumed to be planar. The difference in energy between such a structure and the nonplanar conformer I of a carbocation or *cis*-dihydrodiol should include both electronic and steric effects but notably represents an enthalpy, so that entropic factors are not included.

For the *cis*-dihydrodiols, two minimized conformations as well as a transition structure with planar constraints were calculated by the AM1 semiempirical method. Results are summarized in

(30) Hehre, W. J.; Stewart, R. F.; Pople, J. A. *J. Chem. Phys.* **1969**, *51*, 2657.

(31) (a) Frisch, M. J.; Head-Gordon, M.; Schlegel, H. B.; Raghavachari, K.; Binkley, J. S.; Gonzalez, C.; Defrees, D. J.; Fox, D. J.; Whiteside, R. A.; Seeger, R.; Melius, C. F.; Baker, J.; Martin, R. L.; Kahn, L. R.; Stewart, J. J. P.; Fluder, E. M.; Topiol, S.; Pople, J. A. GAUSSIAN 88, Gaussian, Inc.: Pittsburgh, PA, 1988. (b) We thank J. Douglas Ashbrook for his time and expertise for the installation of computational chemistry code running the IBM-3090. (c) Frisch, M. J.; Head-Gordon, M.; Trucks, G. W.; Foresman, J. B.; Schlegel, H. B.; Raghavachari, K.; Robb, M. A.; Binkley, J. S.; Gonzalez, C.; Defrees, D. J.; Fox, D. J.; Whiteside, R. A.; Seeger, R.; Melius, C. F.; Baker, J.; Martin, R. L.; Kahn, L. R.; Stewart, J. J. P.; Topiol, S.; Pople, J. A. GAUSSIAN 90, Gaussian, Inc.: Pittsburgh, PA, 1990.

(32) Sayer, J. M.; Yagi, H.; Silverton, J. V.; Friedman, S. L.; Whalen, D. L.; Jerina, D. M. *J. Am. Chem. Soc.* **1982**, *104*, 1972.

Chart III

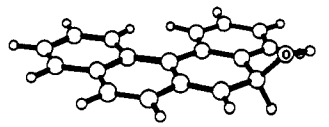

C_6-f Carbocation Derived from BcP-O

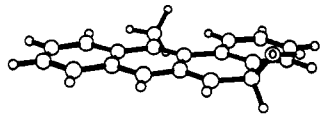

C_6-f Carbocation Derived from 12-MBA-O

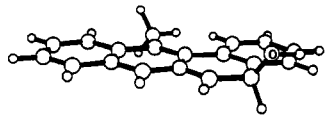

C_6-(f) Carbocation Derived from 12-MBA-O

Table IV. The conformational isomer 5_{ax}, 6_{eq} of the *cis*-dihydrodiol of BcP is ca. 3.5 kcal/mol more stable than the 5_{eq}, 6_{ax} conformer, whereas the 5_{eq}, 6_{ax} conformer is the more stable conformation in the 12-MBA system. In both cases, there is a greater electron–electron repulsion between the oxygen atoms in the higher energy structure due to a decrease in distance between these atoms of 0.04–0.05 Å. In contrast, the NMR results (discussed earlier) showed no thermodynamic preference for either of the two conformations of the *cis*-dihydrodiol dimethyl ethers. The energy differences between the lower energy conformer of the *cis*-dihydrodiol and the planar structure are 11.6 and 9.3 kcal/mol for BcP and 12-MBA, respectively. Notably, however, the planar structure for the 12-MBA *cis*-dihydrodiol has H_1 interdigitated between two of the methyl hydrogens. Rotation of the methyl group by 60° in the planar constrained structure raises the estimated barrier for conformational isomerization of the 12-MBA dihydrodiol from 9.3 to 13.0 kcal/mol, thus reversing the relative barrier heights for the two hydrocarbons. The NMR results in Table III indicate that the energy barrier for conformational isomerization is at least 1.7 kcal/mol higher for the dihydrodiol dimethyl ether of 12-MBA than for the corresponding BcP derivative. This result is consistent with the calculations only if interdigitation of H_1 between the methyl hydrogens does not represent a physically realistic situation. These results suggest that the rotation around C_{12}–CH_3 bond is much faster than the rate of conformational isomerization, and H_1 feels the full steric interaction with the methyl group.

The structures of carbocations C_6-f (the f designates a flat structure) derived from BcP-O and 12-MBA-O were optimized with planar constraints on all atoms of the four rings using AM1 semiempirical[27,28] and STO-3G ab initio[30,31] calculations. All internal coordinates of the substituents at C_5 and C_6 positions were fully optimized. Bond angles and lengths for the calculated structures C_6-f derived from BcP-O and 12-MBA-O at the STO-3G level are given in the supplementary material. Both AM1 and ab initio calculations indicated that the energy difference between C_6-a and the minimized flat structure C_6-f is lower in the 12-MBA system than it is in the BcP system. Carbocations C_6-a derived from BcP-O and 12-MBA-O are ca. 11.4 and 8.6 kcal/mol, respectively, more stable than the corresponding structures C_6-f at the STO-3G basis level (cf. Chart III). As in the case of the model *cis*-dihydrodiol dimethyl ethers, the minimized structure of C_6-f-12-MBA has H_1 interdigitated between two hydrogens of the methyl group. Similar results were obtained for the carbocations using Dewar's AM1 calculations. Rotation of the methyl group by 60° in the planar constrained structure to give C_6-(f) (cf. Chart III) increased the energy barrier from 8.6 to 10.4 kcal/mol for the 12-MBA cation, at the STO-3G basis level. On the basis of the experimental and calculational results for the dihydrodiols and their dimethyl ethers discussed above, we regard this higher estimate for the energy barrier in the 12-MBA system as more reasonable.

These calculations indicate that the energy barriers for the conformational isomerization of the carbocations are *similar to those observed for the cis-dihydrodiols and that the barrier for the conformational isomerization of the C_6 carbocation derived from BcP-O is similar to or somewhat larger than that for the corresponding carbocation derived from 12-MBA-O. Thus, the higher observed yield of phenol from BcP-O relative to 12-MBA-O is probably not caused by any specific electronic stabilization of the planar transition state for k_3 in the case of the BcP carbocation.*

Two remaining possibilities are consistent with the experimental and calculational results. (**1**) The difference in phenol yield may be a reflection of differences in k_4 rather than k_3 in the different hydrocarbon systems, since the ratio of k_4 to k_3, rather than k_3 alone, determines the ratio of solvent adducts to phenol. (**2**) Since the calculated energy barriers reflect only enthalpic (steric and electronic) effects, the existence of a large entropic contribution to the free energy of activation for the conformational isomerization is not ruled out. Differences in the solvation of the two conformations of the carbocation provide a possible source of such entropic effects. It is reasonable to postulate that either k_4 or entropic effects could be sensitive to the structure of the hydrocarbon, resulting in hydrocarbon-specific effects on the ratio of phenols to addition products. This postulate may be justified from the results in ref 11 and Table I for arene oxides in which the K-region is not part of a bay region. Although the two regioisomeric K-region carbocations derived from a given arene oxide have different relative stabilities, the ratio of phenol to addition products is similar for the two carbocations and characteristic of the aromatic system of the hydrocarbon.

Summary and Conclusions for the Acid-Catalyzed Reaction. The results presented in this study and previously[11] for the acid-catalyzed reactions of K-region arene oxides, shown in Figure 1, are consistent with the mechanism proposed in Scheme II. The absence of a deuterium isotope effect on the product distribution indicates that hydride migration and solvent addition do not compete for a common intermediate, and the step that commits the carbocation to phenol formation does not involve hydride migration. That this step is a conformational change is indicated by the observed sensitivity of the phenol yield to local steric hindrance that restricts the orientation of the hydroxyl group and the migrating hydrogen in the hydroxy carbocation intermediate. Specifically, hydroxy carbocations whose hydroxyl group is constrained to be pseudoaxial and whose adjacent (migratory) hydrogen is pseudoequatorial give severely reduced yields of phenolic products. This effect, previously postulated for BA-O's with a substituent peri to the K-region, is shown to be general, in that it is also observed with K-region arene oxides in which the K-region is a part of a bay region, e.g., Chr and BgC.

Nonplanarity of the initially formed carbocation (conformer I), combined with restricted rotation around the biphenyl bond, is an additional factor that reduces the yield of phenols by slowing the rate of conversion of conformer I to II. In model compounds, the K-region *cis*-dihydrodiol dimethyl ethers, the rate of conformational isomerization is slow on the NMR time scale when this rotation is hindered by methyl substitution in the bay region of BA or by the presence of a fjord region in BcP. Consequently, carbocations derived from axial opening of protonated BcP-O or BgC-O were expected to have energy barriers for the conformational isomerization step that were high and similar to the corresponding barriers in the 12-MBA-O system. This should result in low or negligible yields of phenol relative to solvent adducts upon solvolysis of BcP-O or BgC-O. However, contrary

Scheme III

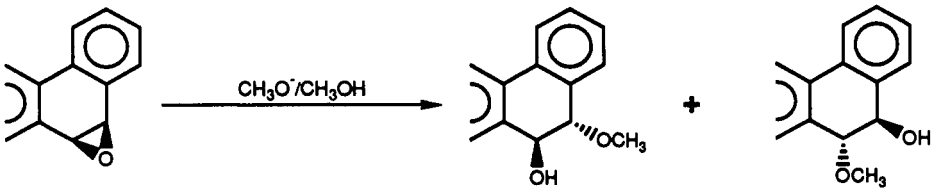

Table V. Rate Constants[a,b] and Product Distributions for the Reaction of Methoxide Ion with K-Region Arene Oxides

arene oxide	$10^5 k_{MeO}$, $M^{-1} s^{-1}$	major product	
		reaction site	%
DMBA-O	127.0	C_6	70
BgC-O	59.7	C_{10}	57
12-MBA-O	53.5	C_6	70
BcP-O	40.9	C_6	70
1-MBA-O	37.8	C_5	51
7-BrBA-O	15.9	C_5	67
7-MBA-O	12.5	C_6	65
4-MBA-O	12.4	C_5	63
11-MBA-O	8.96	C_5	50
3-BrPhe-O	8.86	C_9	52
Chr-O	8.75	C_5	52
BA-O	8.61	C_6	52
DBA-O	8.40	C_6	55[c]
BaP-O	6.73	C_5	51[c]
Phe-O	6.12	C_9	50
Pyr-O	3.39	C_4	50
BeP-O	2.61	C_4	50

[a] At 25 °C in 2% (v/v) acetonitrile in methanol. [b] Standard deviation is 2–7% of the reported value. [c] Product compositions were unchanged after 1, 3, and 6 half-lives.

to expectation, a sizable amount of phenolic products was observed from BcP-O and BgC-O. A significant contribution of hydrocarbon-specific electronic factors that reduce the energy barrier for conformational isomerization of the hydroxy carbocations, as opposed to the *cis*-dihydrodiols, was ruled out by ab initio and AM1 calculations on the carbocations and a putative transition state for their conformational inversion. These calculations showed that the enthalpy of activation for conformational isomerization, which includes electronic as well as steric effects, is similar or somewhat higher for the C_6 cation derived from BcP-O when compared with the activation enthalpy for the analogous cation derived from 12-MBA-O. Alternative explanations for the increased phenol yield from BcP-O relative to 12-MBA-O include specific effects on the competing rate of carbocation capture by solvent (k_4) or entropic contributions to either the k_3 or k_4 step that are not taken into account by the calculations.

Nucleophilic Addition of Methoxide Ion. *trans*-Methanol adducts are the sole products of the reaction of the methoxide ion with K-region arene oxides (Scheme III, Table V). For symmetrical arene oxides such as BeP-O, Phe-O, and Pyr-O, only one regioisomer is possible. As in the case of acid-catalyzed methanolysis (Tables I and II), the reaction rates are sensitive to both electronic and steric effects. Larger aromatic moieties as well as bromine and non-bay-region methyl substitution slightly increase the overall reactivity of the K-region arene oxides with methoxide ion. For example, BA-O and Chr-O are 40% more reactive than Phe-O, and 7-BrBA-O and 7-MBA-O are 85% and 45% more reactive than BA-O. However, the effects of substituents on the reactivities of the individual epoxide centers of the K-region arene oxides are different. With an inductively electron-withdrawing bromine substituent, C_5 and C_6 of 7-BrBA-O are 2.5 and 1.2 times more reactive toward attack by methoxide ion than the corresponding epoxide centers of BA-O. With an electron-donating methyl substituent, C_5 of 4-MBA-O and C_6 of 7-MBA-O are 1.8 times as reactive as the corresponding positions of BA-O, whereas the reactivity of the other epoxide center in these two oxides is relatively unaffected. In a related nucleophilic reaction, the lithium aluminum hydride reduction of para-substituted stilbene oxides,[33] electron releasing substituents were similarly found to favor attack at the α-carbon atom and electron withdrawing substituents to favor attack at the β-carbon atom.

The most striking result in Table V is that the K-region arene oxides that are most reactive toward methoxide ion addition reaction are those whose structures are distorted from planarity (as described in detail above) by the presence of a fjord region or a methyl substituent in a bay-region position. For example, 1-MBA-O and 12-MBA-O are 4–6 times more reactive than BA-O, whereas arene oxides with a methyl substituent that is not in the bay region (e.g., 4-MBA-O and 7-MBA-O) are only 1.4 times more reactive. BcP-O with its fjord region is 6.7 times more reactive than Phe-O toward methoxide ion, whereas BA-O and Chr-O, which contain the same number of aromatic rings as BcP-O, are only 1.4 times more reactive. BgC-O, which may be considered as a derivative of either BcP-O or Chr-O, is only 1.5 times more reactive than BcP-O but is 6.8 times more reactive than Chr-O, which lacks the fjord region. In the nonplanar arene oxides, the structure is distorted by twisting of the biphenyl bond due to steric crowding in a fjord region or in a bay region with a methyl substituent. Relief of this strain on the biphenyl bond, brought about by opening of the epoxide ring and development of normal sp^3 bond angles at the reactive K-region carbon atom, provides a driving force for the reaction. The distorted ground-state structures of these arene oxides may be considered to be closer in energy to their respective transition states compared to the more planar unhindered molecules. Thus, a rate acceleration is anticipated according to the Hammond postulate.[34]

Comparison of the second-order rate constants for the methoxide ion addition reaction at an epoxide center (cf. Table V) to that of acid-catalyzed methanolysis reaction (cf. Table II and ref 11) at the same epoxide center shows a trend such that arene oxides that react faster via the acid-catalyzed pathway also exhibit the faster reaction rates for the methoxide ion addition. Figure 2 shows plots of log $k_{MeO}/k_{MeO}^{Phe\text{-}O}$ vs log $k_H/k_H^{Phe\text{-}O}$ where log k_{MeO} and log k_H are the rate constants for the methoxide ion addition and the acid-catalyzed reaction, respectively, at a single carbon atom of each arene oxide, as calculated from the observed rate constants and the fraction of reaction that occurs at each epoxide center. The data were normalized by dividing by the corresponding rate constants for Phe-O, $k_{MeO}^{Phe\text{-}O}$ and $k_H^{Phe\text{-}O}$. The data of Figure 2 clearly fall into two sets. The first set, which includes all K-region arene oxides except those with a fjord region or a methyl substituent in the bay region, gives a line with a least-squares slope and intercept of 0.33 ± 0.07 and −0.05 ± 0.05, respectively. In contrast, nonplanar arene oxides with a fjord region or a methyl substituent in the bay region exhibit enhanced reactivity with methoxide ion and give another line with a least-squares slope and intercept of 0.31 ± 0.08 and 0.67 ± 0.09, respectively. Although these data exhibit considerable scatter, probably due to the varied structures used and the lack of spread in reactivities among these K-region arene oxides, the line for the twisted arene oxides clearly lies above the line for the planar arene oxides whose bay regions are sterically less congested. *The nonzero intercept of the line corresponding to the twisted arene oxides is a measure of the steric acceleration of the methoxide ion addition reaction in the presence of a crowded bay or fjord region* and corresponds to approximately 0.9 kcal/mol.

As discussed previously, the acid-catalyzed reaction of K-region arene oxides in methanol proceeds via a carbocation mechanism.

(33) Feldstein, A.; VanderWerf, C. A. *J. Am. Chem. Soc.* **1954**, *76*, 1626.
(34) Lowry, T. H.; Richardson, K. S. *Mechanism and Theory in Organic Chemistry*; Harper and Row: New York, 1976; p 102.

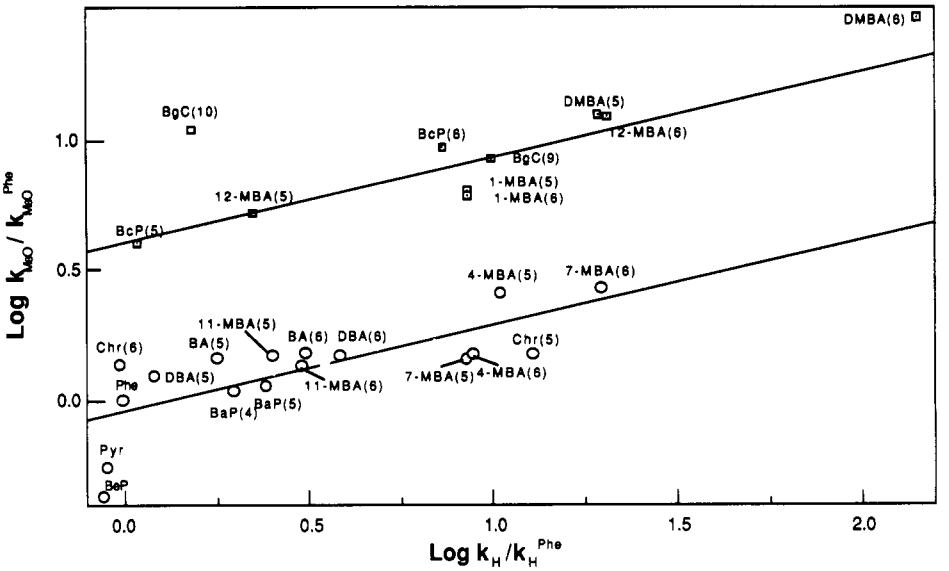

Figure 2. Linear correlation between rates of reactions of K-region arene oxides with methoxide ion and acidic methanol (log k_{MeO} versus log k_H): open circles, planar K-region arene oxides; open squares, nonplanar K-region arene oxides. Abbreviations are for the parent hydrocarbons, and numbers in parentheses indicate the site of reaction of their K-region arene oxides.

The small but statistically significant positive slopes for the two lines in Figure 2 are consistent with a reaction in which epoxide carbon that is attacked by methoxide ion develops a partial positive charge in the transition state, although much less than that for an S_N1 reaction (slope = 1). Thus, in methoxide ion addition, *breaking of the C–O bond of the epoxide must be farther advanced than formation of the new C–O bond to methoxide ion in the transition state.* In related reactions of Phe-O in aqueous solvent, similar transition states with little bond formation to the incoming nucleophile have been proposed on the basis of a small Brønsted β_{nuc} value of 0.2 for sulfur and oxygen nucleophiles and a slightly larger value for nitrogen nucleophiles.[13] A transition state with little bond formation and significant stretching of the C–O bond of the epoxide may be a general feature for nucleophilic addition reactions of benzylic epoxides. The nucleophilic addition of benzylamine to a series of meta- and para-substituted styrene oxides in ethanol was proposed to have a similar transition-state structure,[35] based on the observation of negative Hammett ρ value for methoxide ion attack at the benzylic center. For nucleophilic additions to arene oxides, a direct nucleophilic displacement mechanism (S_N2) or nucleophilic attack on the positive pole of an intimate ion pair has been proposed.[13] Our present results are consistent with an unsymmetrical transition state in which a partial positive charge is developed at the position of attack. It is not possible to determine whether this transition state is reached by partially coupled processes of nucleophilic attack and C–O bond cleavage (S_N2 mechanism) or by prior formation of a dipolar ion derived from C–O cleavage of the epoxide that is then attacked by methoxide ion. In the latter mechanism, the small value of the slopes of the lines in Figure 2 could be a consequence of electrostatic shielding of the positive charge by two nearby negative charges. Previous results with other epoxides have suggested that dipolar ions of this type may in fact be too unstable to have a finite lifetime, i.e., there may be no energy barrier for their collapse to the reactant epoxides.[36,37]

Experimental Section

Materials and Methods. Routine ^1H NMR spectra were measured at 300 MHz in $CDCl_3$ unless otherwise indicated. ^1H–^{13}C NMR correlation spectra were obtained on a modified NT-500 spectrometer.[38,39] Chemical shifts (δ) are reported in parts per million downfield from internal tetramethylsilane and coupling constants (J) are in hertz. UV spectra were measured in methanol. BA-O[40] and its bromo- and methyl-substituted derivatives,[11] BaP-O,[40] BeP-O,[41] partially deuterated (50% deuterated at positions 5 and 8) and undeuterated BcP-O,[20] BgC-O,[23] 3-BrPhe-O,[5] Chr-O,[42] DMBA-O,[40] Phe-O,[40] and Pyr-O[40] were obtained as described. The previously reported DBA-O[43] was prepared by the method of Dansette and Jerina[40] from the *cis*-dihydrodiol in 40% yield. The regioisomeric K-region *trans*-dihydrodiol monomethyl ethers of BgC,[23] Chr,[17] and DMBA[44] were obtained as described. All K-region *cis*-dihydrodiols were known compounds and were synthesized by reaction of the hydrocarbons with osmium tetroxide in pyridine followed by the destruction of the osmate esters with aqueous $NaHSO_3$ as described.[45]

Kinetics. Kinetics of the acid-catalyzed methanolyses and methoxide ion addition reactions were measured spectrophotometrically at 25 °C. Acid-catalyzed reactions were followed by monitoring the decrease in absorption at 273 nm for BaP-O and 262 nm for BeP-O, and by the increase in absorption at 280 nm for BgC-O, 287 nm for BcP-O, 250 nm for 3-BrPhe-O, 271 nm for Chr-O, 293 nm for DBA-O, 246 nm for Phe-O, and 239 nm for Pyr-O. Methoxide ion addition reactions were followed by monitoring the decrease in absorption at 269 nm for BA-O and 1-MBA-O, 348 nm for BgC-O, 253 nm for BcP-O, 273 nm for BaP-O, 7-MBA-O, and 11-MBA-O, 263 nm for BeP-O, 274 nm for 7-BrBA-O, 289 nm for 3-BrPhe-O, 271 nm for Chr-O, 321 nm for DBA-O, 275 nm for DMBA-O, 270 nm for 4-MBA-O, 272 nm for 12-MBA-O, 277 nm for Phe-O, and 299 nm for Pyr-O. HPLC grade methanol was freshly distilled from benzoic acid to remove basic contaminants before use in the acid-catalyzed reaction and was used without further purification for the methoxide ion addition reactions. In a typical measurement, 1 mL of methanol which contained the desired concentration of ethanesulfonic acid or sodium methoxide (25% (wt) solution in methanol, Aldrich) was thermostated at 25 °C for 15 min. Reaction was initiated by addition of substrate in 20 μL of acetonitrile and followed for 8–10 half-lives. The observation of isosbestic points in the time dependent UV spectra for the reaction of arene oxides in acid (0.02–1.2 mM) and in sodium methoxide solution (0.1–4.3 M) indicated that no intermediates accumulated. In all cases, good first-order kinetics were observed. Plots of the pseudo-first-order rate constants versus the concentration of acid or methoxide ion were linear, and the second-order rate constants were estimated from slopes of the lines. Evidence for the

(35) Laird, R. M.; Parker, R. E. *J. Am. Chem. Soc.* **1961**, *83*, 4277.
(36) Sayer, J. M.; Grossman, S. J.; Adusei-Poku, K. S.; Jerina, D. M. *J. Am. Chem. Soc.* **1988**, *110*, 5068.
(37) Islam, N. B.; Gupta, S. C.; Yagi, H.; Jerina, D. M.; Whalen, D. L. *J. Am. Chem. Soc.* **1990**, *112*, 6363.
(38) Bax, A.; Summers, M. F. *J. Am. Chem. Soc.* **1986**, *108*, 2093.
(39) Summers, M. F.; Marzilli, L. G.; Bax, A. *J. Am. Chem. Soc.* **1986**, *108*, 4285.
(40) Dansette, P.; Jerina, D. M. *J. Am. Chem. Soc.* **1974**, *96*, 1224.
(41) Wood, A. W.; Levin, W.; Thakker, D. R.; Yagi, H.; Chang, R. L.; Ryan, D. E.; Thomas, P. E.; Dansette, P. M.; Whittaker, N.; Turujman, S.; Lehr, R. E.; Kumar, S.; Jerina, D. M.; Conney, A. H. *J. Biol. Chem.* **1979**, *254*, 4408.
(42) van Bladeren, P. J.; Jerina, D. M. *Tetrahedron Lett.* **1983**, *24*, 4903.
(43) Harvey, R. G.; Goh, S. H.; Cortez, C. *J. Am. Chem. Soc.* **1975**, *97*, 3468.
(44) Balani, S. K.; Yeh, H. J. C.; Ryan, D. E.; Thomas, P. E.; Levin, W.; Jerina, D. M. *Biochem. Biophys. Res. Commun.* **1985**, *130*, 610.
(45) Baran, J. S. *J. Org. Chem.* **1960**, *25*, 257.

Table VI. NMR Chemical Shifts (300 MHz, $CDCl_3$) of Key Protons in K-Region *cis*- and *trans*-Dihydrodiol Methyl Ether Derivatives

		trans					cis				
		relative	chemical shift (δ, ppm)			$J_{a,b}$,	relative	chemical shift (δ, ppm)			$J_{a,b}$,
hydrocarbon	CH_3O at C	polarity on silica	O-CH_3	CHOCH_3	CHOH	Hz	polarity on silica	O-CH_3	CHOCH_3	CHOH	Hz
BA[a]	5,6							3.39, 3.51	4.50	4.59	2.8
	5	less	3.55	4.34	4.91	7.8	less	3.26	4.30	5.02	3.5
	6	more	3.58	4.42	4.82	7.5	more	3.33	4.42	4.94	3.5
BgC	9	more[b]	3.45	5.25	5.09	2.9		3.14	5.31	5.07	4.1
	10	less[b]	3.38	4.53	5.58	3.0					
BcP	5,6							3.46 br	4.46	4.46	
	5	less	3.61	4.28	4.71	8.8	less	3.36	4.27	4.90	3.2
	6	more	3.66	4.30	4.75	9.5	more	3.37	4.29	4.92	3.3
BaP[a]	4,5							3.41, 3.52	4.86	4.89	3.1
	4	less	3.52	4.75	5.26	6.6	less	3.24	4.66	5.29	3.7
	5	more	3.53	4.77	5.23	6.5	more	3.29	4.69	5.30	3.7
BeP	4		3.50	4.64	5.12	7.1		3.26	4.50	5.20	3.9
7-BrBA	5,6							3.39, 3.77	4.54	5.49	2.2
	5	less	3.30	4.51	5.74	3.3	more	3.74	4.48	5.72	2.9
	6	more	3.48	5.41	4.99	3.3	less	3.39	5.35	4.94	3.4
3-BrPhe	9,10							3.45, 3.35	4.38	4.38	
	9	less	3.61	4.33	4.77	8.3	less	3.25	4.19	4.81	3.7
	10	more	3.59	4.30	4.82	8.3	more	3.28	4.19	4.85	3.7
Chr[c]	5	more	3.44	5.36	5.03	2.9					
	6	less	3.32	4.52	5.66	2.7		3.83	4.61	5.72	3.9
DBA	5,6							3.40, 3.59	4.54	4.70	2.8
	5	less	3.64	4.46	5.08	8.1	less	3.27	4.33	5.11	3.7
	6	more	3.72	4.61	4.94	7.6	more	3.39	4.52	5.00	3.5
DMBA[d]	5,6							3.30, 3.73	4.52	5.14	3.3
	5	less	3.28	4.44	5.32	3.3	more	3.72	4.44	5.32	3.7
	6	more	3.35	5.03	4.96	3.5	less	3.19	4.98	4.86	3.2
1-MBA	5,6							3.2, 3.7 br	4.40	4.53	2.7
	5	less	3.66	4.23	4.82	8.8	less	3.32 br	4.31	4.99	3.2
	6	more	3.73	4.35	4.71	9.3	more	3.45 br	4.45 br	4.90 br	
4-MBA	5,6							3.31, 3.82	4.62	4.97	2.7
	5	more	3.38	4.85	5.09	3.2	less	3.25	4.81	5.00	3.2
	6	less	3.29	4.55	5.21	3.3	more	3.84	4.61	5.28	3.2
7-MBA	5,6		3.27, 3.36	4.54	5.13	3.3		3.29, 3.79	4.54	5.22	2.6
	5	less	3.20	4.41	5.37	3.4	more	3.80	4.51	5.51	2.9
	6	more	3.29	5.04	4.91	3.4	less	3.25	5.07	4.94	3.4
11-MBA	5,6							3.46, 3.57	4.56	4.67	2.9
	5	less	3.62	4.41	5.00	7.8	less	3.33	4.37	5.08	3.4
	6	more	3.65	4.49	4.89	7.8	more	3.33	4.42	4.93	3.4
12-MBA	5,6							3.3, 3.7 br	4.55 br	4.55 br	
	5	less	3.71	4.29	4.73	9.0	less	3.38 br	4.35 br	4.92 br	
	6	more	3.74	4.28	4.77	8.8	more	3.40 br	4.40	4.97	3.0
Phe	9		3.54	4.29	4.75	8.4		3.35	4.29	4.95	3.7
Pyr	4		3.49	4.71	5.20	6.7		3.26	4.59	5.24	3.9

[a] *trans*-Dihydrodiol monomethyl ethers had been previously reported but without NMR data.[18] [b] Results from ref 23. [c] Results from ref 17. [d] Compounds reported without NMR data in ref 44.

insensitivity of the methoxide addition reaction to ionic strength came from the observation that 0.5 M sodium acetate caused no detectable change in the rate of reaction of DMBA-O in 0.5 M sodium methoxide.

Product Analysis. A solution of 1–10 mg of K-region arene oxide in 1–3 mL of acetonitrile was added to 30 mL of 1 mM ethanesulfonic acid or 4 M sodium methoxide in methanol under nitrogen and stirred for 6–8 half-lives at room temperature. Reaction was terminated by addition of 100 mL of ethyl acetate. The ethyl acetate solution was washed several times with water and saturated sodium chloride solution. The water washes from the sodium methoxide reactions were pooled, acidified, and extracted with ethyl acetate, and the two ethyl acetate extracts were combined. Solvent was removed in vacuum and NMR spectra were obtained. Products of the acid-catalyzed reactions consisted of phenols resulting from isomerization of the K-region arene oxides as well as pairs of regioisomeric *cis*- and *trans*-methanol adducts. The amount of K-region phenols formed was determined by integration of the K-region protons ortho to the phenolic hydroxyl groups (cf. Table VIII). These signals are upfield from the aromatic multiplet of the product mixture except in the case of BgC and Chr where the K-region protons are in a bay region and are shifted downfield. Thus, the signals for $H_{1/14}$ and $H_{10/11}$ of the K-region phenols of BgC and Chr, respectively, were utilized (cf. Table VIII). The observation of a doublet at δ 9.70 in the NMR spectrum of the product mixture from the acid-catalyzed reaction of Chr-O indicated the presence of a trace amount of 5-hydroxychrysene (H_4, see below) among the products. For the regioisomeric pairs of *cis*- and *trans*-methanol adducts, integration of the ring carbinol or ether and/or methyl signals allowed quantitation (cf. Table VI). Methoxide ion addition reactions produced only trans addition products, and the ratios between the two products were determined by integration of the NMR signals for the methyl groups of the ethers. Peak areas for these adducts on HPLC (267–270 nm) provided additional confirmation of their ratios. Details of NMR spectra and chromatographic conditions (phenols and addition products) are shown in Tables VI–VIII.

Characterization of Dihydrodiol Monomethyl Ethers. The methoxide ion addition reactions produced only regioisomeric *trans*-dihydrodiol monomethyl ethers, whereas the acid-catalyzed reactions yielded both *cis*- and *trans*-methanol adducts in addition to K-region phenols. Both the *cis*- and *trans*-methanol addition products of Chr-O[17] and DMBA-O[44] and the trans- addition products of BgC-O[23] and 12-MBA-O[19] were previously characterized by spectroscopic methods. Other dihydrodiol monomethyl ethers were separated by HPLC on a silica column (cf. Table VII) prior to characterization. In all cases, chemical ionization mass spectra (CI, NH_3) showed molecular ions at $(M + NH_4)^+$ with base peaks corresponding to loss of water or methanol. Several NMR and chemical methods, described below, were used for the structural assignment of the methyl ethers. Table VI summarizes the NMR chemical shifts of key protons and their coupling constants for the *cis*- and *trans*-dihydrodiol monomethyl ethers and selected *cis*-dihydrodiol dimethyl ethers.

The observation of coupling constants in the range of 7–10 Hz between the carbinol proton and the ring ether proton in the NMR spectra of the trans addition products from the reaction of BA-O, BaP-O, BcP-O, BeP-O, 3-BrPhe-O, DBA-O, 1-MBA-O, 11-MBA-O, 12-MBA-O, Phe-O, and Pyr-O allowed unambiguous assignment of *trans*-pseudodiequa-

Table VII. Chromatographic Separation of K-Region Phenols and Dihydrodiol Mono- and Dimethyl Ethers

hydrocarbon	phenolic fraction k'	*cis*-dimethyl ether k'	dihydrodiol monomethyl ether isomer	cis k'	trans k'	column[a]	solvent[b]
BcP	3.17	2.53	5-CH_3O, 6-HO	5.16	3.17	1	A
			5-OH, 6-CH_3O	5.76	3.50		
BaP	2.25	1.83	4-CH_3O, 5-HO	2.62	3.84	1	B
			4-HO, 5-CH_3O	2.79	4.06		
BeP	3.29		4-CH_3O, 5-HO	3.81	5.36	1	B
BgC	2.02		9-CH_3O, 10-HO	2.93	9.57	1	C
			9-HO, 10-CH_3O		6.29		
3-BrPhe	1.71	1.95	9-CH_3O, 10-HO	2.99	3.00	1	C
			9-HO, 10-CH_3O	3.70	3.28		
Chr	2.74		5-CH_3O, 6-HO		10.56	1	B
			5-OH, 6-CH_3O	6.89	7.88		
DBA	0.34	1.21	5-CH_3O, 6-HO	1.89	3.37	1	D
			5-OH, 6-CH_3O	2.64	4.04		
Phe	0.48		9-CH_3O, 10-HO	2.63	2.94	2	E
Pyr	2.80		4-CH_3O, 5-HO	3.51	5.44	1	B

[a] Column 1, Du Pont Zorbax SIL column (0.94 × 25 cm); column 2, Rainin silica column (1 × 25 cm). [b] Solvent A, 0.5% methanol and 2.5% ethyl acetate in hexane; solvent B, 1% methanol and 3% ethyl acetate in hexane; solvent C, 0.5% methanol and 5% ethyl acetate in hexane; solvent D, 0.05% methanol in dichloromethane; solvent E, 0.2% methanol in dichloromethane.

Table VIII. NMR Chemical Shifts (300 MHz, $CDCl_3$) of Key Protons of K-Region Phenols

phenol	chemical shifts (δ, ppm) ortho[a]	others
4-HO-BaP	7.23, H_5	8.98 (d, J = 9.3, H_{11}), 8.95 (d, J = 6.8, H_{10}), 8.41 (d, J = 9.3, H_3), 8.28 (s, H_6)
5-HO-BaP	7.17, H_4	8.98 (m, H_{10}, H_{11}), 8.84 (s, H_6)
5-HO-BcP	6.99, H_6	9.04 (d, J = 8.3, $H_{1/12}$), 8.95 (d, J = 8.3, $H_{1/12}$), 8.35 (d, J = 7.9, H_4)
6-HO-BcP	7.07, H_5	9.02, (d, J = 8.3, $H_{1/12}$), 8.93 (d, J = 8.3, $H_{1/12}$), 8.23 (d, J = 9.0, H_7)
4-HO-BeP	7.36, H_5	8.97 (d, J = 7.8, 1 H), 8.85 (m, 2 H), 8.76 (dd, J = 1.7, 7.3, 1 H) for H_1, H_8, H_9, and H_{12}
10-HO-BgC	7.84, H_9	8.88 (m, $H_{1/14}$), 8.75 (m, $H_{1/14}$)
9-HO-3-BrPhe	6.98, H_{10}	8.72 (s, H_4), 8.58 (d, J = 7.4, H_5), 8.31 (dd, J = 1.9, 7.5, H_8)
10-HO-3-BrPhe	7.02, H_9	8.79 (d, J = 1.8, H_4), 8.50 (dd, J = 1.6, 7.4, H_5), 8.19 (d, J = 8.8, H_1)
6-HO-Chr	8.00, H_5	8.75 (d, J = 8.1, $H_{4/10}$), 8.62 (d, J = 9.0, H_{11}), 8.60 (m, $H_{4/10}$), 8.41 (dd, J = 1.3, 7.9, H_7), 7.84 (d, J = 9.0, H_{12})
5-HO-DBA	7.22, H_6	9.07 (s, H_{14}), 8.94 (s, H_7), 8.35 (dd, J = 1.4, 8.0, H_4)
6-HO-DBA	7.03, H_5	9.64 (s, H_7), 9.24 (s, H_{14})
9-HO-Phe	7.02, H_{10}	8.70 (d, J = 8.6, $H_{4/5}$), 8.59 (dd, J = 2.2, 8.0, $H_{4/5}$), 8.32 (dd, J = 1.7, 7.8, H_8)
4-HO-Pyr	7.37, H_5	8.53 (d, J = 7.8, H_3), 8.23 (d, J = 8.0, 1 H)

[a] The singlet K-region proton ortho to the phenolic hydroxyl group.

torial stereochemistry for the oxygen containing groups. *trans*-Pseudodiaxial adducts and *cis*-pseudoaxial–pseudoequatorial adducts both displayed coupling constants of 2–4 Hz for these protons. This caused difficulty in assignment of cis versus trans stereochemistry for the adducts from 7-BrBA-O, BgC-O, 4-MBA-O, and 7-MBA-O oxides since steric factors force these trans adducts into pseudodiaxial conformations. Similar difficulties were encountered in the assignment of the methanol adducts from Chr-O[17] and DMBA-O.[44] For each of these oxides there is either a bulky peri-substitute adjacent to the K-region or the K-region is a part of hindered bay region. Since the cis and trans adducts, including positional isomers from each arene oxide, were separable by HPLC, comparison of retention times for these adducts with those for the monomethyl ethers produced by partial methylation of *cis*-dihydrodiols permitted distinction between the trans pseudodiaxial adducts and the cis pseudoaxial–pseudoequatorial adducts. Partial methylation of *cis*-dihydrodiols with limiting methyl iodide in the presence of sodium hydride produced both possible monomethyl ethers in addition to the dimethyl ethers. The K-region *cis*-dihydrodiol monomethyl ethers of BA and several BA derivatives are included as the same methodology was used for their structural characterization.

The structural assignment of one of each pair of the *cis*- and *trans*-dihydrodiol monomethyl ethers of 11-MBA, the *cis*-dihydrodiol monomethyl ethers of BA, BaP, 3-BrPhe, DBA, 4-MBA, and 12-MBA, was based on COSY and NOE difference experiments. As expected, the carbinol proton and the ring ether proton showed NOE interactions with the aromatic protons in the peri position. In addition, NOE interaction is observed between the methoxy methyl protons and the ring ether proton. The structural assignment of one of each pair of the *trans*-dihydrodiol monomethyl ethers of BA, BaP,[46] 3-BrPhe, and DBA were made based upon a combination of COSY and ^{1}H-detected multiple bond ^{1}H-^{13}C correlation (HMBC[38,39]). These experiments provided sufficient information for complete and unambiguous ^{1}H and ^{13}C resonance assignments (data not shown). Structural assignments were confirmed by selective ^{1}H–^{1}H NOE difference experiments as described above.

The K-region *trans*-dihydrodiol monomethyl ethers of BcP were characterized by the methanolysis of the partially deuterated K-region arene oxide, 50% deuterated at C_5 and C_8. As expected, the carbinol proton (OH coupled) is downfield from the ring ether proton in both cases. The NMR signal for H_6 in these monomethyl ethers appears as unsymmetrical triplet (50% doublet, $J_{5,6}$ = 9 Hz, 50% singlet) which is twice as intense as the H_5 doublet.[14]

The K-region *cis*-dihydrodiol monomethyl ethers of 1-MBA were converted in quantitative yield to the known K-region phenol methyl ethers of 1-MBA[11] with BF_3-etherate.[44] The early eluting isomer on a silica gel HPLC column produced only 1-methyl-5-methoxybenz[*a*]anthracene whereas the late eluting isomer produced only 1-methyl-6-methoxybenz[*a*]anthracene. Thus, the early and late eluting *cis*-dihydrodiol monomethyl ethers were assigned as the 5-methoxy-6-hydroxy and 5-hydroxy-6-methoxy isomers, respectively.

Structural assignments of the *cis*- and *trans*-monomethyl ethers of 7-BrBA, 4-MBA, and 7-MBA dihydrodiols were made by comparison of their NMR spectra with those of the corresponding dihydrodiols. Protons which are peri to a ring substituent are shifted downfield by 0.4–0.5 ppm.[11,47] Methylation of either carbinol results in an expected upfield shift (0.2–0.4 ppm). Thus, for the methyl ether in which the methoxy group is peri to a ring substituent, the difference in chemical shifts between the ring ether and carbinol protons must be smaller than the difference between the two carbinol protons of the dihydrodiol. The opposite positional isomer of the methyl ether displays a larger difference between these signals than does the dihydrodiol. Structural assignments of *cis*-dihydrodiol monomethyl ethers of 4-MBA were confirmed by selective ^{1}H–^{1}H NOE difference spectra. Also, catalytic reduction (10% Pd on carbon in methanol, 1 atm of H_2, stirred 3 h at room temperature) of the monomethyl ethers of the 7-BrBA dihydrodiols produced the expected methyl ethers of the BA dihydrodiols.

The results in Table VI show that the methyl protons of a pseudoequatorial methoxy group are edge deshielded by about 0.4 ppm relative to the pseudoaxial methoxy group. NMR spectra of the isomeric K-region pseudodiaxial *trans*-dihydrodiol monomethyl ethers of DMBA show methyl ether signals at δ 3.28 and 3.35 ppm. NMR signals for the methyl ether groups of *cis*-5-pseudoequatorial–6-pseudoaxial dihydrodiol

(46) *trans*-Dihydrodiol monomethyl ethers of BA and BaP have been previously characterized by chemical transformation.[18] The spectroscopic assignments are in agreement with what have been reported previously.

(47) Jeffrey, A. M.; Blobstein, S. H.; Weinstein, I. B.; Beland, F. A.; Harvey, R. G.; Kasai, H.; Nakanishi, K. *Proc. Natl. Acad. Sci. U.S.A.* **1976**, *73*, 2311.

dimethyl ether are at δ 3.30 and 3.73. Also, the *cis*-dihydrodiol monomethyl ethers of DMBA show NMR resonances for the methoxy methyl at δ 3.72 and 3.19 for the 5-methoxy and 6-methoxy isomers, respectively. Thus, the low field signal at ca. δ 3.7 is assigned to the pseudoequatorial methoxy methyl, whereas the high field signal at ca. δ 3.2 is assigned to the pseudoaxial methoxy methyl. The same observation can be made on comparing the methoxy methyl signals of the *cis*-methyl ethers of 7-BrBA, 4-MBA, and 7-MBA.

A minor product obtained from the acid-catalyzed methanolysis of BgC-O, chromatographically distinct from the trans methanolysis products, has an NMR spectrum similar to that of the *trans*-9-methoxy-10-hydroxy isomer but different from that of the *trans*-9-hydroxy-10-methoxy isomer. The ring ether proton H_9, δ 5.31, is downfield from the carbinol proton H_{10}, δ 5.07 (OH coupled), due to the edge deshielding effect of the bay region. Thus, this adduct was assigned the structure *cis*-9-methoxy-10-hydroxy BgC. Since the K-region of BgC is a part of a bay region, the *cis*-dihydrodiol monomethyl ether must have a 9-pseudoaxial-10-pseudoequatorial conformation for the oxygen substituents. The observed NMR chemical shift of δ 3.14 for the methoxy methyl group confirmed the pseudoaxial position of the methoxy group and the structural assignment.

K-Region Phenols. With the exception of the phenolic products from BcP, phenols eluted earlier from the silica column than did methanol adducts (cf Table VII). K-region phenols of BcP co-chromatographed with the early eluting trans addition products under conditions described in Table VII. In each case, the phenolic fractions were isolated and characterized by spectroscopic methods. Expected red shifts of their UV spectra were observed on addition of a small amount of base (sodium methoxide) in all cases. Mass spectra (CI, NH_3) showed ions at $(M + NH_4)^+$ and MH^+, the latter often being larger. Structures of the K-region phenols were assigned by comparing NMR spectra of the phenolic fraction with that of authentic samples of pure phenols or known mixtures of isomeric K-region phenols.

K-region phenols of BaP,[48] 6-hydroxychrysene (obtained as the acetate esters from Aldrich) and Phe (Aldrich) were known compounds. A mixture of the known K-region phenols of DBA[49] (9:1) was obtained on treatment of the *cis*-dihydrodiol with 40% trifluoroacetic acid in dichloromethane for 30 min at room temperature. The phenolic fraction obtained from the reaction products of BeP-O, BgC-O, and Pyr-O contained only one K-region phenol which was characterized by spectroscopic methods. The phenolic products of 3-BrPhe were compared to authentic phenols obtained as described below. Table VIII summarizes the NMR spectra for the phenolic products.

Acid-catalyzed reaction of Chr-O in acetonitrile produced the K-region phenols in a ratio of 3:97. Treatment of the phenolic mixture with diazomethane produced the corresponding phenol methyl ethers which were separated on a silica column (Axxiom-silica, 0.94 × 25 cm) eluted with 10% dichloromethane in hexane at a flow rate of 10 mL/min. The minor early (3%) eluting isomer, $k' = 2.24$, is 5-methoxychrysene: HRMS calculated for $C_{19}H_{14}O$, 258.1044; found, 258.1035; UV λ_{max} (10% CH_2Cl_2 in hexane) 266; NMR δ 9.72 (dd, J = 7.8, 1.2, H_4), 8.67 (d, J = 9.1, H_{11}), 8.64 (dd, J = 8.9, 1.4, H_{10}), 7.97 (d, J = 9.1, H_{12}), 7.92 (dd, J = 6.9, 1.8), 7.82 (dd, J = 6.9 & 2.4), 7.45–7.65 (m, 4), 7.51 (s, H_6), 4.16 (s, 3 H). The multiplet at δ 9.72 corresponding to H_4 is diagnostic of a bay-region phenol[48,49] or its methyl ether. This compound was identical to the only methyl ether obtained from the reaction of *trans*-5-methoxy-6-hydroxydihydro-Chr with BF_3-etherate (4 h at room temperature, 5% 5-methoxychrysene and 95% 6-hydroxychrysene). The major late eluting isomer ($k' = 2.36$) is 6-methoxychrysene.[43] NMR δ 8.67 (d, J = 8.2, $H_{4/11}$), 8.63 (d, J = 8.3, $H_{4/11}$), 8.56 (d, J = 9.0, H_{11}), 7.89 (s, H_5), 7.81 (d, J = 9.0, H_{12}), 4.17 (s, 3 H).

K-Region Phenols of BcP. A mixture of the previously reported K-region phenols of BcP[50] was obtained by dehydration of the K-region *cis*-dihydrodiol of BcP in 50% trifluoroacetic acid in dichloromethane. NMR of the product mixture showed a ratio of 98:2 of the K-region phenols. Due to the instability of the minor phenol, the mixture was immediately methylated with diazomethane. The resulting methyl ethers were chromatographed on Du Pont Zorbax SIL column (0.94 × 25 cm) eluted with 5% dichloromethane in hexane. The minor early eluting isomer (2%, $k' = 3.81$) is identical to the phenol methyl ether (the only product) obtained from the treatment of *trans*-5-hydroxy-6-methoxydihydro-BcP with 50% BF_3-etherate in ether for 60 h at room temperature:[44] NMR δ 9.11 (d, J = 8.0, $H_{1/12}$), 9.01 (d, J = 7.9, $H_{1/12}$), 8.37 (d, J = 8.8, H_7), 8.02 (dd, J = 2.6 & 7.7, H_9), 7.93 (d, J = 8.8, H_8), 7.5–7.7 (m, 4 H), 7.18 (s, H_5), 4.14 (s, 3 H). The NMR assignment is based on comparison with the previously reported NMR assignment of BcP and 5-BrBcP[51] and the expected downfield shift for the hydrogen (H_7) peri to the methoxy group.[11] In addition, the assignment of the doublet at 8.37 ppm to H_7 is further confirmed by the observation of an unsymmetrical triplet for that proton in the NMR of the dehydration product of the dihydrodiol monomethyl ether 50% deuterated at C_5 and C_6. HRMS calculated for $C_{19}H_{14}O$ 258.1045, found 258.1047. The major-late eluting isomer (98%, $k' = 4.10$) is identical to the only product obtained from the dehydration of *trans*-5-methoxy-6-hydroxydihydro-BcP with 50% BF_3-etherate in ether for 60 h: NMR δ 9.08 (d, J = 8.4, $H_{1/12}$), 9.01 (d, J = 8.5, $H_{1/12}$), 8.47 (dd, J = 1.5 & 8.0, H_4), 7.96 (dd, J = 1.1 & 7.9, H_9), 7.80 (d, J = 8.6, H_8), 7.72 (d, J = 8.6, H_7), 7.4–7.7 (m, 4 H), 7.06 (s, H_6), 4.11 (s, 3 H); HRMS calculated for $C_{19}H_{14}O$ 258.1045, found 258.1047. Thus, the minor and major phenols are assigned the structures of 6-hydroxy- and 5-hydroxy-BcP, respectively.

K-Region Phenols of 3-BrPhe. Treatment of the *cis*-dihydrodiol (10 mg) of 3-BrPhe with 10 mL of 50% trifluoroacetic acid in dichloromethane for 1 h at room temperature produced a mixture of the K-region phenols in a 1:2 ratio. The two phenols were separated on a silica HPLC column (Rainin-Microsorb, 1 × 25 cm) eluted with 0.5% methanol and 10% dichloromethane in hexane. The minor early eluting ($k' = 3.56$) and the major-late eluting isomer ($k' = 3.75$) were O-methylated with methyl iodide and sodium hydride in dry tetrahydrofuran. The methylations were completed after 18 h as indicated by the disappearance of the starting phenol on HPLC. Standard workup provided the isomeric K-region methyl ethers in quantitative yield. The phenol methyl ether obtained from the minor-early eluting phenol was identical to the only product obtained from *trans*-9-hydroxy-10-methoxydihydro-3-BrPhe on dehydration with BF_3-etherate as described previously.[44] This phenol methyl ether was assigned the structure 3-bromo-10-methoxyphenanthrene based on this result. This structural assignment is further supported by the observation of a well resolved doublet of doublets for H_2 δ 7.68 coupled to both H_1 δ 8.22 (J = 8.8), shifted downfield by the peri 10-methoxy group[11] and the bay-region H_4 δ 8.77 (J = 1.9): MS (CI, NH_3) m/z 287, 289 $(M + H)^+$; NMR δ 8.77 (d, J = 1.8, H_4), 8.49 (d, J = 7.4, H_5), 8.22 (d, J = 8.8, H_1), 7.77 (d, J = 7.5, 1 H), 7.68 (dd, J = 1.9 & 8.8, H_2), 7.4–7.5 (m, 2 H), 6.99 (s, H_9), 4.08 (s, CH_3). Similarly, the major late eluting phenol produced a phenol methyl ether that was identical to the only product obtained by dehydration of the 9-CH_3O, 10-HO *trans*-dihydrodiol methyl ether. 3-Bromo-9-methoxyphenanthrene: MS (CI, NH_3) m/z 287, 289 $(M + H)^+$; NMR δ 8.70 (s, H_4), 8.55 (d, J = 7.7, H_5), 8.35 (dd, J = 1.7 & 8.3, H_8), 7.6–7.7 (m, 4 H), 6.93 (s, H10), 4.09 (s, CH_3). Thus, the minor early and the major late eluting phenols were assigned the structures 10-hydroxy and 9-hydroxy 3-BrPhe, respectively.

Methylation of K-Region Dihydrodiols with Methyl Iodide. Dihydrodiol methyl ethers were obtained from dihydrodiols by partial methylation with limiting methyl iodide as described previously.[17] In a typical synthesis, 50 mg of sodium hydride (57% suspension in mineral oil) was added to 2 mL of freshly distilled tetrahydrofuran containing 20 mg of the dihydrodiol and 1 equiv of methyl iodide under nitrogen. The reaction was followed by HPLC, until 60–70% of the dihydrodiol was converted to products. Standard workup and chromatography (cf. Table VII) provided the two possible dihydrodiol monomethyl ethers, dihydrodiol dimethyl ether and the unreacted dihydrodiol.

Supplementary Material Available: Figures showing geometries of both conformational isomers a and b of the C_5 and C_6 carbocations derived from BcP-O, the flat conformation of carbocation C_6-f derived from BcP-O and 12-MBA-O, and the flat conformation C_6-(f) in which the methyl group of structure C_6-f derived from 12-MBA-O is rotated by 60° based on calculation at the STO-3G level (4 pages). Ordering information is given on any current masthead page.

(48) Yagi, H.; Holder, G. M.; Dansette, P. M.; Hernandez, O.; Yeh, H. J. C.; LeMahieu, R. A.; Jerina, D. M. *J. Org. Chem.* **1976**, *41*, 977.
(49) Platt, K. L.; Oesch, F. *J. Org. Chem.* **1982**, *47*, 5321.
(50) Newman, M. S.; Blum, J. *J. Am. Chem. Soc.* **1964**, *86*, 503.
(51) Bax, A.; Ferretti, J. A.; Nashed, N.; Jerina, D. M. *J. Org. Chem.* **1985**, *50*, 3029.